THE BELL SYSTEM TECHNICAL JOURNAL
Vol. 53, No. 8, October 1974
Printed in U.S.A.

Theory of the Single-Material, Helicoidal Fiber

By J. A. ARNAUD

(Manuscript received March 29, 1974)

The theory of propagation in a new single-material, single-mode, optical fiber is given. The modes are of the whispering-gallery type, with the propagation taking place along helicoidal paths close to the boundary of a cylindrical dielectric rod. The beams are confined in the azimuthal direction in helicoidal ridges. It is shown that single-mode, low-loss operation is possible if the helix period is of the order of the rod cross-section area divided by the wavelength and the ridge area is of the order of 1 percent of the rod cross-section area for two channels. The rod is supported by helicoidal wings that play a role in the mode-selection mechanism.

I. INTRODUCTION

The best-known single-mode optical fiber is the clad fiber. If the difference in refractive index between core and cladding is small, single-mode propagation can be achieved for core diameters that are large compared with the wavelength. It is, however, desirable to use just one material, such as quartz, that exhibits low impurity and scattering losses. In a previous work,[1] we indicated that single-mode propagation could be achieved in a single-material configuration that we called a "helicoidal fiber." Figure 1 represents a more recent version of this type of fiber.

To explain the mechanism of operation, let us consider first a cylindrical dielectric rod with radius $a = \rho$. The refractive index of the rod is perhaps $n = 1.45$ (quartz), and the surrounding medium is air. Waves are guided along the rod boundary as shown in Fig. 2a. These so-called "whispering-gallery modes" can be represented by rays repeatedly reflected from the boundary because of total reflection. In the interior of the rod, the modes are described by Bessel functions $J_\nu(kr) \times \exp(i\nu\phi)$, where ν is a large integer and kr is a large number of the order of ν. Because kr and ν are both large and comparable to one

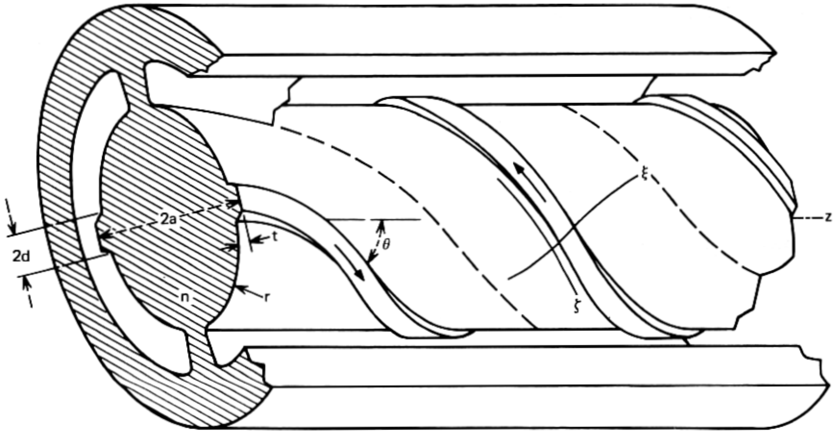

Fig. 1—Open view of the single-material, helicoidal fiber for two optical channels. The two optical beams propagate in the two ridges shown, with areas $t \times 2d$. The helicoidal motion is essential to maintain confinement. High-order modes are not confined. They radiate away to the envelope through the wings (only part of one is shown). The ratio period/diameter is much larger than that shown in the figure.

another, the Bessel functions can be approximated by Airy functions. The field is oscillatory from the rod boundary down to a slightly smaller radius r_c called the caustic (or turning point) radius. For radii smaller than r_c, the field decays exponentially. Thus, the field of whispering-gallery modes clings tightly to the rod boundary. The distance between the caustic and the boundary, which defines in some sense the "thickness" of the mode, is for the fundamental mode of the order of $(\lambda^2 a)^{\frac{1}{3}}$, with λ the wavelength in the medium and a the rod radius. For example, if $\lambda = 1\ \mu\text{m}$ and a is equal to 8 mm, the fundamental mode thickness is of the order of $20\ \mu\text{m}$. It increases with the mode number m, approximating as $m^{\frac{2}{3}}$. As m increases, the phase velocity increases too.

These whispering-gallery modes can be generalized to take into account a motion along the rod axis z. The combined rotation and axial motion results in a helicoidal path that can be understood from simple ray-optics considerations. The only significant difference from the previous case is that the radius a of the rod should be replaced, in the expression for the mode thickness, by the helix radius of curvature, $\rho = a/\sin^2\theta$, where θ denotes the angle that the helix makes with the rod axis. For example, if a is $80\ \mu\text{m}$ and $\theta = 0.1$ radian, the mode thickness is the same as in the previous example, where a was assumed to be $8000\ \mu\text{m}$. If θ is equal to zero, there is of course no confinement

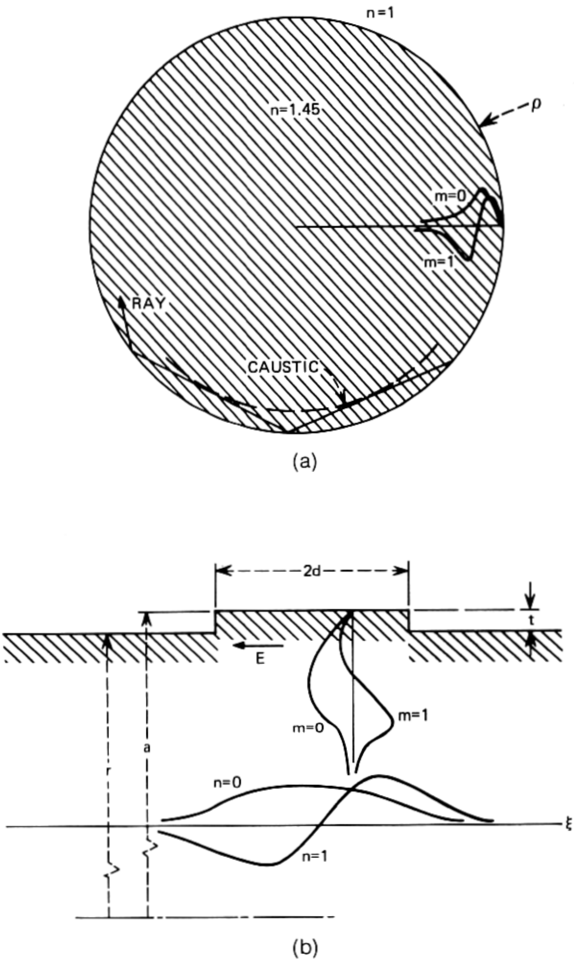

Fig. 2—(a) Whispering-gallery modes clinging to a circular boundary with effective radius $\rho\,(=a/\sin^2\theta)$. The field ($m = 0, 1, \cdots$) is described exactly by Bessel functions and approximately by Airy functions. (b) Cross section in a local r, ξ plane.

near the rod boundary. Observation of helicoidal rays in optics has been reported.[2]

Let us now assume that we have selected a convenient value for θ, perhaps $\theta = 2.5°$, and that we wish to define one or more channels in the azimuthal direction. This can be achieved with helicoidal separators,[1] or ridges, as shown in Fig. 1, that follow the path of the desired whispering-gallery modes. It is clear, intuitively, that the optical power will tend to remain in the ridges. As the mode number increases, either in the azimuthal or radial direction, the modes occupy larger and larger volumes and eventually "spill out" of the ridges. Because there is maximum confinement in the ridge when $\theta = \pi/2$ and no confinement at all when $\theta = 0$, it is plausible that only a single mode remains confined in the ridge for a proper choice of θ. The higher-order modes radiate away from the ridge along the boundary. They can be absorbed easily without degrading the fundamental mode. In this paper, we justify the above intuitive arguments and show that strong discrimination against unwanted modes can indeed be obtained.

The first step of the calculation is to obtain the propagation constants of whispering-gallery modes in circular cylinders in a convenient form. This is done in Section II. In Section III, we investigate the case of helicoidal boundaries in the local mode approximation and obtain the design parameters. In Section IV, the case of small ridges is investigated with the help of a new perturbation method.

The single-material helicoidal fiber discussed in this paper can be compared to the single-material ridge guide recently demonstrated[3] and analyzed.[4,5] These two single-material fibers have features in common. The mode-selection mechanism rests on similar general principles. It can be ascribed to a coupling between ridges carrying trapped modes and two-dimensional substrates carrying radiation modes.[6] In the case of the ridge guide, the slab constitutes the two-dimensional substrate needed to ensure single-mode propagation. In the case of the helicoidal fiber, the dielectric rod itself can be considered a two-dimensional mode sink because the whispering-gallery modes that it guides have a restricted thickness in the radial direction, as we have discussed before. In both cases, a good discrimination against high-order modes should in principle be obtained by increasing the distance between the absorbing elements and the ridges, because these elements are coupled through the radiation field rather than through evanescent waves.

The theory given in this paper is applicable to purely metallic helicoidal waveguides as well as to dielectric waveguides. The metallic helicoidal waveguide is attractive as a low-loss, multichannel, single-mode system for long-distance microwave communication. It can be compared to the groove guide[7] shown in Fig. 4c. The metallic helicoidal waveguide has the advantage that TEM modes are absent. In the groove guide, any lack of symmetry between the two plates introduces a large loss through coupling to the (slower) TEM modes. This is, in fact, also the reason for the superiority of the dielectric ridge guide[4] over the metallic groove guide.[7]

II. PROPAGATION OF WHISPERING-GALLERY MODES IN CYLINDRICAL SURFACES

Let us consider a circular dielectric cylinder with radius a. For E modes, the ϕ and z components of the electric field have the form

$$E(r, \phi, z) = J_\nu(ur/a) \exp [i(\nu\phi + k_z z], \tag{1}$$

where

$$u^2 \equiv (k^2 - k_z^2)a^2. \tag{2}$$

Assuming that the discontinuity in refractive index is sufficiently large, a condition well satisfied for quartz rods in air, the boundary condition at $r = a$ is

$$J_\nu(u) = 0, \tag{3}$$

because, for the type of mode considered, the field tends to vanish at the boundary. The zeros of J_ν are denoted $u_m(\nu)$, $m = 0, 1, 2, \cdots$.

We introduce new coordinates ξ, ζ in place of y, z (see Fig. 1)

$$\begin{aligned} \xi &= r \cos\theta\, \phi - \sin\theta\, z, \\ \zeta &\equiv \cos\theta\, z + r \sin\theta\, \phi, \end{aligned} \tag{4}$$

where

$$\theta \equiv \tan^{-1} (2\pi r/p), \tag{5}$$

the quantity p, for "period," being for the moment an arbitrary constant. The wave numbers Γ_ξ, Γ_ζ in the new coordinate system are related to ν, k_z by

$$\nu = r \cos\theta\, \Gamma_\xi + r \sin\theta\, \Gamma_\zeta, \tag{6a}$$

$$k_z = -\sin\theta\, \Gamma_\xi + \cos\theta\, \Gamma_\zeta. \tag{6b}$$

They are such that

$$\Gamma_\xi \xi + \Gamma_\zeta \zeta \equiv \nu\phi + k_z z. \tag{6c}$$

The characteristic equations, (2) and (3), are now written, using eqs. (6),

$$(-\sin\theta\, \Gamma_\xi + \cos\theta\, \Gamma_\zeta)^2 a^2 + u_m^2(r \cos\theta\, \Gamma_\xi + r \sin\theta\, \Gamma_\zeta) = k^2 a^2. \tag{7}$$

Equation (7) provides us with the desired relation between Γ_ζ and Γ_ξ. We wish to simplify this relation. Because we are interested in whispering-gallery modes corresponding to large values of ν, we can use the

Table I — Values of b parameter in eq. (10)

m	b_m	$[3\pi(2m + 3/4)/2^{1/2}4]^{2/3}$ (J.W.K.B.)
0	1.85575	1.841
1	3.24461	3.239
2	4.38167	4.379
3	5.387	5.385

following approximation for $u_m(\nu)$[8]

$$u_m(\nu) = \nu + b_m \nu^{1/3}, \tag{8}$$

where b_m is given in Table I. In the second column in Table I, the J.W.K.B. approximation for b_m obtained from simple ray optics considerations is given. As we can see, the error does not exceed 1 percent even for small m.

We note further that a is not very different from r. Thus, we set $a = r + t$, $t \ll r$. Because we are considering waves that do not depart very much from the reference helicoidal path, Γ_ζ is very close to k, and the transverse wave number Γ_ξ is small compared with Γ_ζ. Neglecting products of small quantities, (7) becomes

$$\Gamma^2 \equiv \Gamma_\zeta^2 + \Gamma_\xi^2 = k^2[1 + 2t/\rho - 2b_m(k\rho)^{-2/3}], \tag{9}$$

where we have introduced the reference helix curvature $\rho = a/\sin^2\theta$. The term $2t/\rho$ expresses the fact that, at the reference radius r, the phase velocity is smaller than at the boundary with radius a. The term $2b_m(k\rho)^{-2/3}$ results from the radial variation of the field. The larger the radial mode number m, the smaller the tangential wave number Γ. Note that the system is approximately isotropic.

III. HELICOIDAL BOUNDARY

In the previous section we have assumed that the boundary is a circular cylinder with radius a. We now assume that a is a function of ξ, but that it remains independent of ζ. By letting a vary with ξ, we generate a helicoidal surface. Azimuthal confinement of the whispering-gallery beams can be expected for various well-shaped profiles $a(\xi)$. For simplicity, we assume here that $a(\xi) = a$, a constant, for $-d < \xi < d$, and $a = r$, where r denotes the reference radius, anywhere else in the period. A slightly tapered transition region is assumed. Mode mixing can therefore be neglected in the evaluation of the propagation constants of the modes $m = 0, 1, 2, \cdots$. A small amount of mode mixing is nevertheless needed for this mode-selection mechanism to operate.[4–7]

From (9), the wave numbers for the fundamental mode ($m = 0$) and first-order mode ($m = 1$) in the ridge (unprimed number) and outside the ridge (primed number) are, respectively,

$$\Gamma_0^2 = k^2[1 + 2t/\rho - 2b_0(k\rho)^{-\frac{2}{3}}], \tag{10a}$$

$$\Gamma_{0'}^2 = k^2[1 - 2b_0(k\rho)^{-\frac{2}{3}}], \tag{10b}$$

$$\Gamma_1^2 = k^2[1 + 2t/\rho - 2b_1(k\rho)^{-\frac{2}{3}}], \tag{10c}$$

$$\Gamma_{1'}^2 = k^2[1 - 2b_1(k\rho)^{-\frac{2}{3}}]. \tag{10d}$$

The axial wave numbers $\Gamma_{\zeta 0}$ and $\Gamma_{\zeta 1}$ for the two modes 0 and 1 are now obtained using the standard dielectric slab theory. If we normalize the axial wave number $\Gamma_{\zeta 0}$ by defining

$$K^2 \equiv (\Gamma_{\zeta 0}^2 - \Gamma_{0'}^2)/(\Gamma_0^2 - \Gamma_{0'}^2) \tag{11}$$

and introduce the V parameter

$$V^2 \equiv (\Gamma_0^2 - \Gamma_{0'}^2)d^2, \tag{12}$$

we have, for the modes $m = 0$, an explicit relation between V and K,

$$V = \{\tan^{-1}[K(1 - K^2)^{-\frac{1}{2}}] + n\pi/2\}(1 - K^2)^{-\frac{1}{2}}, \tag{13}$$

where $n = 0, 2, 4, \cdots$ correspond to even modes and $n = 1, 3, \cdots$ to odd modes.* A similar relation holds for the modes $m = 1$, $n = 0, 1, 2, \cdots$.

The axial wave numbers $\Gamma_{\zeta mn}$ of these various modes m,n are plotted in Fig. 3 as functions of the ridge width $2d$, for $\lambda = 1\ \mu m$, $n = 1.45$ (quartz), a rod radius $a = 50\ \mu m$, and a ridge height $t = 3.5\ \mu m$. We have chosen $\theta = 2.5°$, corresponding to a helix radius of curvature $\rho = 25$ mm. Modes whose axial wave number is less than $\Gamma_{0'}$ (the wave number of the fundamental mode outside the ridge) suffer radiation losses.

This figure clearly shows that only one mode ($m = 0$, $n = 0$) is free of radiation loss if $2d$ is less than 14 μm. For $2d = 14\ \mu m$, the field of the fundamental mode decays in azimuth by a factor of $1/e$ at a distance

$$\xi_0 = (\Gamma_{\zeta 0}^2 - \Gamma_{0'}^2)^{-\frac{1}{2}} = 6.3\ \mu m \tag{14}$$

on either side of the ridge. For two channels, the "wings" holding the

---

* The mode number n should not be confused with the refractive index n.

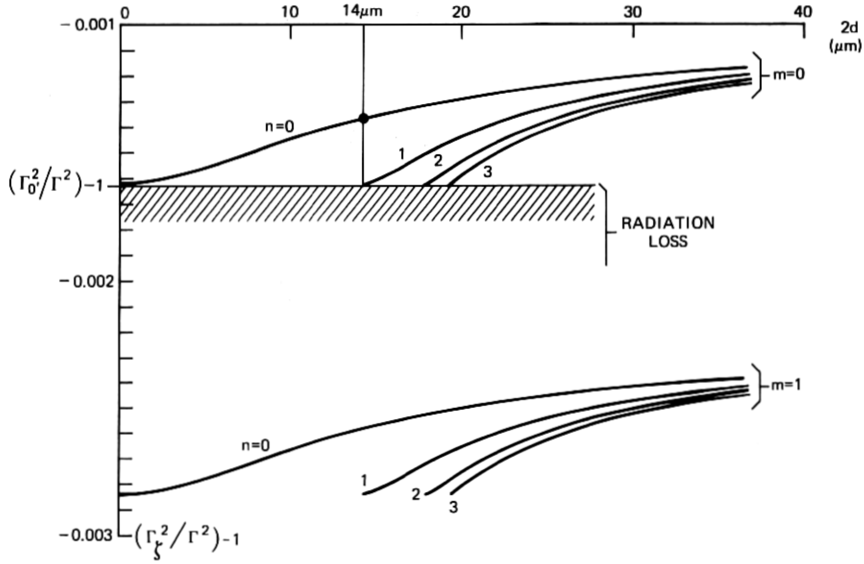

Fig. 3—Axial wave numbers $\Gamma_{\zeta mn}$ for various m and n modes (r and ξ coordinates). Radiation loss is suffered whenever $\Gamma_\zeta < \Gamma_{0'}$. The radiation zone is shaded. This figure shows that single-mode propagation is possible if the ridge width $2d$ is less than 14 μm (for $\lambda_0 = 1$ μm, $n = 1.45$, $t = 3.5$ μm, $a = 50$ μm, and $\theta = 2.5°$).

rod in Fig. 1 are located at a distance $\pi a/2 = 80$ μm from the corrugation. At that distance, the field has decayed by a factor of more than 10^5. The fundamental mode therefore suffers negligible radiation loss (bending losses are not considered here). If we set the condition that ξ_0 be $\frac{1}{10}$ of $\pi a/4$, we obtain the approximate condition $\theta \approx \lambda/a$ for single-mode low-loss operation. More detailed relations are given at the end of Section IV.

The local mode theory used in this section is expected to be applicable when the ridge width $2d$ is large compared to the ridge height, t, and large compared to the wavelength, λ. In the next section, we find that a perturbation method applicable to small ridge areas ($2\ td$) leads to almost identical conclusions.

IV. LINE PERTURBATION OF SURFACE WAVES

We give a general theory of the trapping of surface waves by rods of small cross section. This theory is then applied to helicoidal ridges of small cross section.

Let us consider an isotropic surface, perhaps an inductive surface, supporting a plane wave with wave number k. Let us introduce a di-

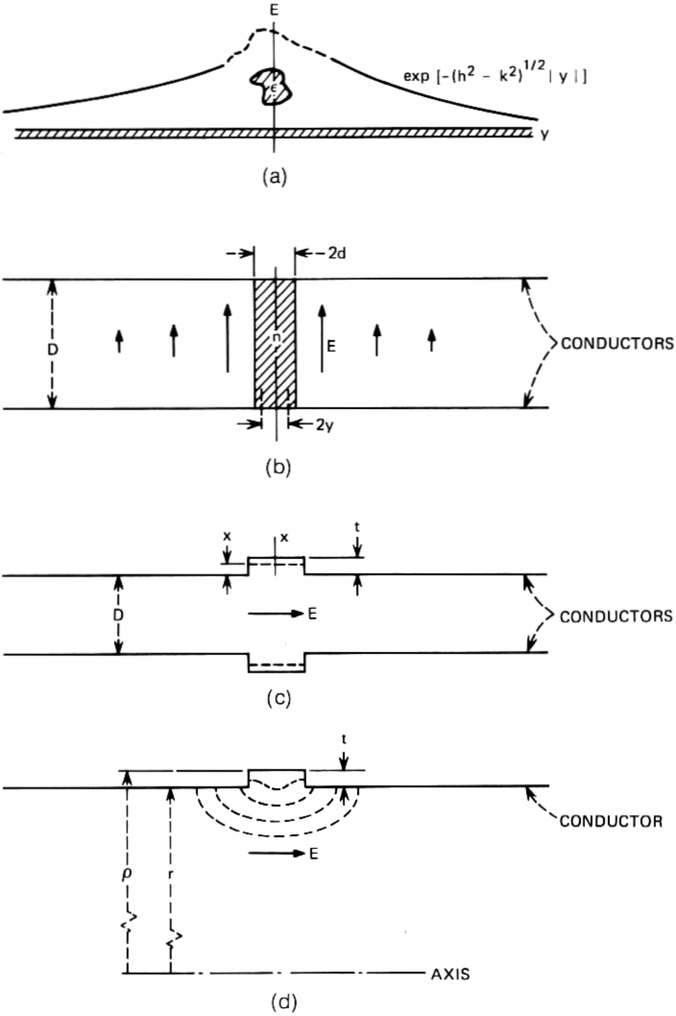

Fig. 4—Various methods of introducing a line perturbation on a surface wave. (a) Reactive (e.g., corrugated) surface perturbed by a dielectric rod. (b) TEM waves perturbed by a dielectric slab. (c) "Groove guide."[7] (d) Ridge guide considered in this paper. The torsion of the helicoidal motion is not essential. The radius of curvature ρ of the helix is the important parameter that determines mode selection.

electric rod of very small cross section parallel to this surface, some distance away from it (Fig. 4a). Because the power carried by the plane wave is infinite, a straightforward application of the conventional perturbation method does not give any meaningful result. Therefore, we shall proceed the other way around. We start from the perturbed state and assume that we know the propagation constant $h > k$. The wave is in that case confined transversely with a decay rate $(h^2 - k^2)^{\frac{1}{2}}$. We now "peel off" the rod and evaluate the successive perturbations until the perturbation resulting from the rod vanishes. By specifying that $h \rightarrow k$ in that limit, the initial value of h is obtained.

For simplicity, this method is first explained for the case where $\epsilon \approx \epsilon_0$, the perturbed field being of the order of the unperturbed field. Let σ be a parameter such that $\sigma = 0$ corresponds to the absence of the rod and $\sigma = 1$ corresponds to the presence of the rod. Furthermore, σ is so chosen that, in the perturbation formula

$$dh/d\sigma = \alpha(h^2 - k^2)^{\frac{1}{2}}, \tag{15}$$

α is a constant. This can be done because we have factored out a term $(h^2 - k^2)^{\frac{1}{2}}$ inversely proportional to the power carried by the mode. (The distortion of the field in the close neighborhood of the rod does not contribute significantly to the total power, because of the large transverse extent of the field.) The ratio σ is essentially the ratio of the present cross-section area of the perturbating rod to its original cross-section area. Integrating eq. (15) from $\sigma = 1$ to $\sigma = 0$, we obtain

$$\int_k^h (h^2 - k^2)^{-\frac{1}{2}} dh = \alpha \tag{16a}$$

or

$$h = k \cos \alpha \approx k(1 - \alpha^2/2). \tag{16b}$$

To clarify the significance of this result, let it be applied to a configuration where the exact solution is known. Consider two parallel perfectly conductive plates with spacing D carrying TEM modes, as shown in Fig. 4b. If we introduce a dielectric slab with $\epsilon \approx \epsilon_0$ and width $2d$, we obtain the so-called "H-guide" configuration proposed by Tischer.[9] (Note, however, that we consider here the H modes rather than the low-loss modes.) The parameter $\sigma = y/d$, where y is shown in Fig. 4b, clearly satisfies the requirements set up above. The conventional perturbation formula (see, for example, Ref. 5, Part II, eq. (21), with $\mathbf{E}_p \approx \mathbf{E}$, $\mathbf{H}_p \approx \mathbf{H}$, $\mathbf{E}^\dagger = \mathbf{E}$, $\mathbf{H}^\dagger = -\mathbf{H}$) is

$$\Delta h = \tfrac{1}{2}\omega \int (\epsilon - \epsilon_0) E^2 dS \Big/ \int \mathbf{E} \times \mathbf{H} \cdot \mathbf{d}S. \tag{17}$$

For our case, we obtain, taking into account the $\exp\left[-(h^2 - k^2)^{\frac{1}{2}}|y|\right]$

dependence of the field on y,

$$dh/d\sigma = (\mu_0/\epsilon_0)^{\frac{1}{2}}(h^2 - k^2)^{\frac{1}{2}}(\epsilon - \epsilon_0)\omega d \equiv \alpha(h^2 - k^2)^{\frac{1}{2}}. \quad (18)$$

Thus the constant α is, from (18),

$$\alpha = (n^2 - 1)kd, \quad (19)$$

where $\epsilon/\epsilon_0 \equiv n^2$. Application of (16b) now gives the perturbed wave number h

$$h = k[1 + \tfrac{1}{2}(n^2 - 1)^2k^2d^2]. \quad (20)$$

The exact solution to the problem, for small $(n^2 - 1)kd$, is well known [see, for example, Ref. 5, Part II, footnote after eq. (11)]. We have, with the approximation $\tan [(n^2 - 1)^{\frac{1}{2}}kd)] \approx (n^2 - 1)^{\frac{1}{2}}kd$,

$$h^2 - k^2 = (n^2 - 1)^2k^4d^2. \quad (21)$$

Equation (21) coincides with our perturbation result, (20), because $h \approx k$. Having satisfied ourselves with the validity of our perturbation technique, we apply it to a small wall perturbation. We assume that the case of quartz in air is the same as the case of a metallic boundary, except for the wavelength λ/n replacing λ.

For a wall perturbation with cross-section area s, the perturbation formula is

$$\Delta h = \tfrac{1}{2}\omega\mu_0 H^2 s \Big/ \int \mathbf{E} \times \mathbf{H} \cdot \mathbf{d}S, \quad (22)$$

if the electric field is equal to zero. Note that h increases if the volume is increased, e.g., if we introduce corrugations in the wall.

For H waves uniform along the y-axis (see Figs. 4c and 4d) ($E_y \equiv E$), we have, from Maxwell's equations,

$$H_x = -(k/\omega\mu_0)E, \quad (23a)$$

$$H_z = (i\omega\mu_0)^{-1}\partial E/\partial x. \quad (23b)$$

Substituting in (22) we obtain the perturbation

$$\Delta h = (s/2k)(\partial E/\partial x)^2(h^2 - k^2)^{\frac{1}{2}} \Big/ \int E^2 dx. \quad (24)$$

Defining σ as x/t (see Figs. 4c or 4d), the constant α defined in (15) is found to be

$$\alpha = (s/2k)(\partial E/\partial x)^2 \Big/ \int E^2 dx, \quad (25)$$

the derivative being evaluated at the first zero of $E(x)$ for the mode $m = 0$, the second for the mode $m = 1$, and so on.

For whispering-gallery modes, we have

$$E = \mathrm{Ai}(t), \tag{26a}$$

where Ai( ) denotes the Airy function and

$$t \equiv (2k^2/\rho)^{\frac{1}{3}}x - (2k^2/\rho)^{-\frac{2}{3}}(k^2 - h^2), \tag{26b}$$

ρ being the boundary radius. Substituting in eq. (25), we obtain

$$\alpha = 2f_m ktd/\rho, \tag{27}$$

where f_m is a numerical factor

$$f_m = (d\mathrm{Ai}/dt)^2_{t=t_m} \Big/ \int_{-\infty}^{t_m} \mathrm{Ai}^2(t)dt, \tag{28}$$

$t_0, t_1, \cdots, t_m, \cdots$ being the zeros of $\mathrm{Ai}(t)$. By numerical integration, we find

$$f_0 = 0.981\cdots \tag{29a}$$

$$f_1 = 0.955\cdots. \tag{29b}$$

Thus, the change in propagation constant resulting from a wall deformation of area $s \equiv 2td$ is, from (27),

$$h_m - k = \tfrac{1}{2}f_m^2 k^3 s^2/\rho^2. \tag{30}$$

As long as the perturbation is small, h_1 remains smaller than $\Gamma_{0'}$ and only the mode $m = 0$ is free of radiation loss. For a sufficiently large perturbation, however, h_1 may exceed $\Gamma_{0'}$. Then the modes $m = 0$ and $m = 1$ are both free of radiation loss, that is, the system is no longer single-mode. The condition for the system to be single-mode is therefore

$$h_m - \Gamma_{1'} < \Gamma_{0'} - \Gamma_{1'},$$

or

$$f_m^2 k^3 s^2/\rho^2 < 2k(b_0 - b_1)(k\rho)^{-\frac{2}{3}}. \tag{31}$$

$\Gamma_{0'}$, $\Gamma_{1'}$, and the constants b_0, b_1 were defined in Section III. The above condition can be written, using the values in Table I for b_0, b_1,

$$k^2 s < 1.74(k\rho)^{\frac{2}{3}}. \tag{32}$$

If we take the limit $d \rightarrow 0$ in the expressions given in Section III, we obtain instead

$$k^2 s < 1.68(k\rho)^{\frac{2}{3}}, \tag{33a}$$

which is very close to the perturbation result, (32). Thus, the local mode approach and the perturbation approach agree closely, not only in form, but also numerically. Because $\rho \approx a/\theta^2$, θ being the angle that the helix makes with the z axis, and $\theta \approx 2\pi a/p$, p being the helix period, condition (33) for single-mode operation can be rewritten

$$s < 0.012(\lambda^2 p^2/a)^{\frac{2}{3}}. \tag{33b}$$

The extent ξ_0 in azimuth of the fundamental mode, defined as the $1/e$ point of the field, $\xi_0 = (h_0^2 - k^2)^{-\frac{1}{2}} \approx (2k)^{-\frac{1}{2}}(h_0 - k)^{-\frac{1}{2}}$, is, from (30) with $m = 0$, given by

$$k\xi_0 \approx \rho/ks. \tag{34a}$$

If we specify that the fundamental mode field has decayed by a factor of 10^5 at the "wings," located, for two channels (see Fig. 1), a distance $\pi a/2$ away from the ridge, we must have $\xi_0 = (\pi a/2)/11.5$. Introducing the helix period p, this condition for the fundamental mode to have small radiation loss can be written

$$s > 0.005(\lambda p/a)^2. \tag{34b}$$

The condition for a single mode to propagate, (33b), and for the fundamental mode to have small radiation losses, (34b), are consistent if

$$p < 5a^2/\lambda. \tag{35}$$

For example, if $a = 50\ \mu m$, $\lambda = (1/1.45)\ \mu m$, according to eq. (35), the helix period, p, must be smaller than 18 mm. A period of 10 mm, for instance, would be quite adequate. Note that for such rather long periods the optical path is not significantly increased by the circular motion. Radiation into free space is negligible, as long as the medium surrounding the ridge is air. For mechanical reasons, however, we may want to use a material with lower index. In that case, radiation into the surrounding medium may be a limitation.

V. CONCLUSION

The single-material helicoidal fiber proposed earlier by the author has been shown to support only one mode, with low radiation loss, provided the following two conditions are satisfied:

Helix period $\approx$ rod cross-section area/wavelength.
Ridge area $\approx$ rod cross-section area/70.

More detailed calculations, similar in spirit to the ones given in Ref. 5, would be necessary to specify the magnitude of the radiation losses and the exact value of the mode discrimination. The helicoidal fiber, like any single-mode fiber with large mode cross section, may be sensitive to bending losses. The bending loss is therefore another key point that needs to be investigated.

REFERENCES

1. J. A. Arnaud, "Note on the Use of Whispering-Gallery Modes in Communication," unpublished work, September 1971.
2. F. G. Reick, "The Optical Whispering Mode of Polished Cylinders and its Implications in Laser Technology," Appl. Opt., 1965, 4, pp. 1395–1399.
3. P. Kaiser, E. A. J. Marcatili, and S. E. Miller, "A New Optical Fiber," B.S.T.J., *52*, No. 2 (February 1973), pp. 265–269.
4. E. A. J. Marcatili, "Slab-Coupled Waveguides," B.S.T.J., *53*, No. 4 (April 1974), pp. 645–674.
5. J. A. Arnaud, "Transverse Coupling in Fiber Optics—Part II: Coupling to Mode Sinks," B.S.T.J., *53*, No. 4 (April 1974), pp. 675–696; "Part III: Bending Losses," B.S.T.J., *53*, No. 7 (September 1974), pp. 1379–1394.
6. J. A. Arnaud, "Selection of Waveguide Modes by Two-Dimensional Mode Sinks," Topical Meeting on Integrated Optics, New Orleans, Louisiana, January 21–24, 1974, Digest of Tech. Papers, p. WB12.1.
7. F. J. Tischer, "The Groove Guide, a Low-Loss Waveguide for Millimeter Waves," IEEE J. of Microwave Theory and Techniques, *11*, 1963, p. 291. The equivalent resonator problem ($k^2 - k_z^2 \rightarrow k^2$) is treated in: L. A. Weinstein, *Open Resonators and Open Waveguides*, Boulder, Colorado: The Golem Press, 1969, p. 87 and Fig. 20b; the mode selection mechanism is discussed by T. Nakahara and N. Kurauchi in *Advances in Microwaves*, L. Young, ed., New York: Academic Press, 1969.
8. *Royal Society Mathematical Tables*, Bessel Functions, Vol. 7, Part 3, Cambridge, England: Cambridge University Press, 1960, p. 18.
9. F. J. Tisher, "The H Guide, a Waveguide for Microwaves," I.R.E. Conv. Record, 1956, Microwaves Inst., Part 5, p. 44.